PHYSICAL REVIEW VOLUME 174, NUMBER 1 5 OCTOBER 1968

Ground-State Energy Eigenvalues and Eigenfunctions for an Electron in an Electric-Dipole Field[*]

J. E. Turner and V. E. Anderson[†]
Health Physics Division, Oak Ridge National Laboratory, Oak Ridge, Tennessee 37830
and
Kenneth Fox[‡]
Department of Physics and Astronomy, The University of Tennessee,
Knoxville, Tennessee 37916, *and Space Sciences Division,*
Jet Propulsion Laboratory, Pasadena, California 91103

(Received 12 April 1968; revised manuscript received 10 June 1968)

Ground-state energy eigenvalues and eigenfunctions are obtained by a variational method for an electron in the field of a finite, stationary, permanent electric dipole. The dipole moments studied cover the range from the minimum value required for binding ($D_{\rm min} = 0.6393\ ea_0$) to $D = 400\ ea_0$, where the system is equivalent to the hydrogen atom perturbed slightly by a distant stationary negative charge. The eigenvalues obtained agree with those reported by Wallis, Herman, and Milnes, who determined them by another method in the range $D = 0.84\ ea_0$ to $30\ ea_0$. The normalized eigenfunctions display the manner in which the electronic charge density changes from that of the hydrogen atom at very large D to a flat distribution approaching that which is characteristic of a zero-energy continuum state as the minimum moment is approached from above. Optimized variational wave functions for different values of D are presented for use in other calculations. Contour maps and profiles of electronic charge density are shown for a number of values of D. Mean values of the powers -1, 1, and 2 of the distances of the electron from the dipole charges are also calculated.

I. INTRODUCTION

The motion of an electron in an electric-dipole field has been considered recently as a model for low-energy electron scattering by polar molecules[1-11] and ion pairs in semiconductors,[12] and for color-center problems.[13,14] Experimental results on the drift of electron-swarms through polar gases[15,16] led to the suggestion that electrons might be temporarily captured into loosely bound states through rotational excitation of polar molecules.[16] Wallis, Herman, and Milnes[14] have calculated binding energies for an electron in the field of a finite, stationary, permanent electric dipole for values of dipole moment D between $0.84\ ea_0$ and $30\ ea_0$ (e = electronic charge and a_0 = radius of first Bohr orbit in hydrogen). Until more recent work it was not known whether a model[5] invoking the existence of a bound state in a dipole field would apply to molecules with arbitrarily small dipole moments.

Analysis of the electron-dipole system by the WKB method[17] indicated that a minimum dipole moment is required to bind an electron, and a preliminary variational calculation[4,18] showed that a bound state exists for D as small as $0.6495\ ea_0$. After these results were found, several investigators[7,19-21] showed that the minimum dipole moment required for binding an electron is $D_{\rm min} = 0.6393\ ea_0$ ($= 1.625 \times 10^{-18}$ esu cm).[22] Some experimental evidence from electron-swarm data has been presented[23] in support of this conclusion. The properties of excited states of the electron in the dipole field have also been studied.[24,25]

We calculate below by means of a variational technique the lowest energy eigenvalue for dipole moments ranging from $D_{\rm min} = 0.6393\ ea_0$ to $D = 400\ ea_0$.[26] Our method differs from that of Ref. 14 and will be described in detail. We also calculate ground-state energy eigenfunctions for a number of values of D. These functions are applicable in calculations of cross sections for electron capture and for scattering involving intermediate bound states.[5,6]

The ground-state motion of a bound charged particle in the field of a stationary electric dipole has intrinsic interest as a quantum-mechanical system. Classically, there is always a bound state for an arbitrarily small dipole moment.[27,28] The calculations below show the manner in which the electronic charge density behaves as the minimum dipole moment is approached from above.

In the following sections we discuss the forms of variational functions used in our calculations, the elements of the Hamiltonian and normalization matrices, the methods of obtaining the energy eigenvalues and eigenfunctions, and the numerical results. Contour maps and profiles of the electronic charge distributions about the dipole are also presented.

II. VARIATIONAL WAVE FUNCTIONS

In Fig. 1 we represent the finite, stationary, permanent electric dipole by charges $\pm q$ located at fixed points $z = \pm R/2$. The dipole moment is $D = qR$. The position of an electron of charge $-e$ and mass m is determined by its distances r_1 and r_2 from the charges $\pm q$ and by the azimuthal angle about the z axis. The Schrödinger equation is separable in elliptic-hyperbolic coordinates defined by

$$\xi = (r_1 + r_2)/R \text{ and } \eta = (r_1 - r_2)/R. \tag{1}$$

The ranges of the variables are $1 \leq \xi \leq \infty$ and $-1 \leq \eta \leq 1$, negative values of η corresponding to posi-

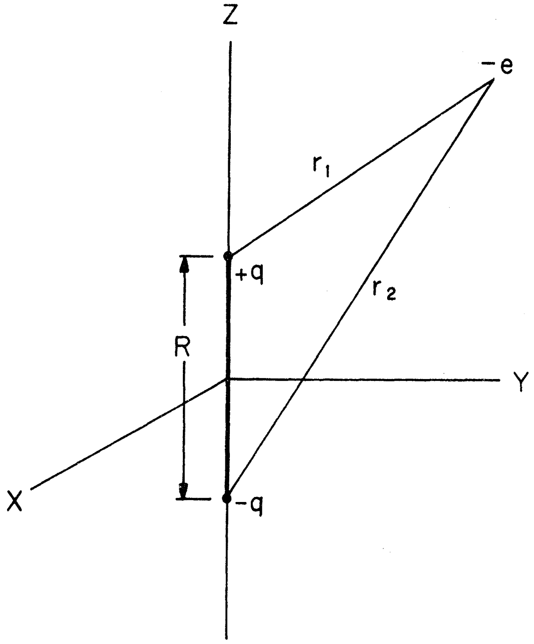

FIG. 1. Coordinate system for an electron in the field of a dipole.

tive values of z. Surfaces of constant ξ and η are, respectively, ellipsoids and hyperboloids of revolution about the z axis.

We used two forms for the trial function in calculating ground-state energy eigenvalues. First, we used the trial function previously employed by us[20] to calculate the minimum dipole moment, $D_{\min} = 0.6393$, required for binding an electron:

$$\psi(\xi,\eta) = e^{-\frac{1}{2}\alpha\xi^t} \sum_{p,q=0}^{\infty} C_{pq}\xi^p\eta^q . \tag{2}$$

Here the adjustable parameters are α, t, and the C_{pq}. This expansion is appropriate for low values of D, where letting α and, more importantly, t be small extends the wave function out to large distances from the dipole. The exponential term in Eq. (2) thus characterizes states with small binding energies. We used Eq. (2), which we shall call the low-D expansion, in the range $D_{\min} \leq D \leq 2$.

A second, high-D, expansion[29]

$$\begin{aligned}\psi(\xi,\eta) &= e^{-\alpha r_1/R} \sum_{p,q=0}^{\infty} C_{pq}\xi^p\eta^q \\ &= e^{-\frac{1}{2}\alpha(\xi+\eta)} \sum_{p,q=0}^{\infty} C_{pq}\xi^p\eta^q \end{aligned} \tag{3}$$

was used in the range $2 \leq D \leq 40$. Here coefficients C_{pq} and α are the adjustable parameters. In the limit as $R \to \infty$ and with $q = e$ the electron and the positive charge of the dipole form the hydrogen atom. As a numerical check on the results obtained with Eq. (3), we expect, therefore, at large D that

$$\psi(\xi,\eta) \to \pi^{-\frac{1}{2}} e^{-r_1/a_0} . \tag{4}$$

Thus, as shown below, we find in the numerical calculations that $\alpha \to R$, $C_{00} \to 1/\sqrt{\pi} = 0.564\,190$, $C_{pq} \to 0$ for $p, q \neq 0$, and that the energy eigenvalue $\lambda \to -e^2/2a_0 = -1$ Ry. Poor results were obtained with Eq. (3) for $D \lesssim 2$. Both the high- and low-D expansions were used in the range $2 \leq D \leq 5$, where they gave the same results.

III. MATRIX ELEMENTS

We shall outline the calculation of the matrix elements for the low-D trial function. Details for this and other trial functions can be found elsewhere.[30]

The kinetic-energy operator for the electron is[31]

$$T = -\frac{\hbar^2}{2m}\nabla^2 = -\frac{2\hbar^2}{mR^2(\xi^2-\eta^2)}\left\{\frac{\partial}{\partial\xi}\left[(\xi^2-1)\frac{\partial}{\partial\xi}\right] + \frac{\partial}{\partial\eta}\left[(1-\eta^2)\frac{\partial}{\partial\eta}\right]\right\} . \tag{5}$$

Its potential energy in the field of the electric dipole, as depicted in Fig. 1, is

$$V = qe(1/r_2 - 1/r_1) = 4De\eta/R^2(\xi^2-\eta^2) . \tag{6}$$

We write the trial function (2) in the form

$$\psi(\xi,\eta) = \sum_{p,q=0}^{\infty} C_{pq}\phi_{pq} \tag{7}$$

$$\text{where } \phi_{pq} = e^{-\frac{1}{2}\alpha\xi^t}\xi^p\eta^q . \tag{8}$$

The elements of the kinetic-energy matrix, representing the differential operator in Eq. (5), are given by

$$T_{pq,ij} = -(\hbar^2/2m)\int \phi_{pq}\nabla^2\phi_{ij}\,d\tau \tag{9}$$

where $d\tau = \pi R^3(\xi^2-\eta^2)d\xi d\eta/4$ is the volume element in elliptic-hyperbolic coordinates, including a factor of 2π from integration over the azimuthal angle. We find that

$$\begin{aligned} T_{pq,ij} &= (\pi R\hbar^2/4m)\tfrac{1}{2}[1+(-1)^{q+j}] \\ &\times (q+j+1)^{-1}\{2e^{-\alpha} + [-(p-i)^2+1+t(p+i+1)]I_{p+i} \\ &+ [(p-i)^2-1-t(p+i-1)]I_{p+i-2} \\ &+ 8jqI_{p+i}/(q+j-1)\} . \end{aligned} \tag{10}$$

$$\text{Here } I_r \equiv \int_1^\infty e^{-\alpha\xi^t}\xi^r d\xi , \tag{11}$$

and use has been made of the identity $\alpha t I_{p+i+t} = e^{-\alpha} + (p+i+1)I_{p+i}$. The elements of the potential-energy and normalization matrices are

$$V_{pq,ij} = \frac{2\pi DeRI_{p+i}}{q+j+2}\,\frac{1+(-1)^{q+j+1}}{2} \tag{12}$$

and

$$N_{pq,ij} = \frac{\pi R^3}{2}\,\frac{1+(-1)^{q+j}}{2}\left(\frac{I_{p+i+2}}{q+j+1} - \frac{I_{p+i}}{q+j+3}\right). \tag{13}$$

To calculate the ground-state energy eigenvalue for a given value of D, we use the determinantal equation

$$\det(T+V-\lambda N)=0 \tag{14}$$

and find the smallest value of λ that results when α and $\beta(\equiv 1/t)$ are varied. By the variational theorem, this value gives an upper bound to the true ground-state energy eigenvalue for the value of D chosen. Repeating this procedure with determinants of increasing rank gives a sequence of values of λ that converges to the true ground-state energy eigenvalue from above. The coefficients C_{pq} in Eq. (7) are then calculated for this value of λ.

We see from Eqs. (10)–(13) that, for a given value of D,

$$\mu \equiv \tfrac{1}{4}\lambda R^2 \tag{15}$$

rather than the energy λ, is the quantity actually determined.

IV. NUMERICAL RESULTS

A summary of numerical results is contained in the accompanying tables and figures. Details of the calculations and numerical cross-checks are given in Ref. 30. It is believed that the values of λ as a function of D are accurate to within ±2 in the last digit shown.

In Tables I and II we summarize the energy eigenvalues and variational parameters for the complete range of dipole moments. The results in Table I were obtained with the low-D expansion (2) and those in Table II with the high-D expansion (3). With the variational parameters optimized, both forms of the trial function give about the same rate of conver-

TABLE I. Energy eigenvalues λ and optimized variational parameters α and β obtained with low-D expansion (2) and dipole charge $q=e$.

D (ea_0)	$-\mu$	$-\lambda$ (Ry) This calculation	$-\lambda$ (Ry) Wallis *et al.*[a]	Rank	α (For rank 15)	β (For rank 15)
0.639 315	0	0	...	4[b]	∞	∞
0.667 0	1.000×10^{-20}	8.973×10^{-20}	...	36	1.83	6.23
0.674 65	$1.000\,0\times10^{-16}$	$8.777\,9\times10^{-16}$	...	36	1.54	5.08
0.692 72	$1.000\,0\times10^{-12}$	$8.334\,6\times10^{-12}$	...	36	1.32	4.00
0.723 65	$1.000\,0\times10^{-9}$	$7.635\,0\times10^{-9}$	...	36	1.18	3.19
0.740 99	$1.000\,0\times10^{-8}$	$7.284\,9\times10^{-8}$	...	36	1.15	2.93
0.764 49	$1.000\,0\times10^{-7}$	$6.843\,7\times10^{-7}$	...	36	1.12	2.68
0.797 368	$1.000\,00\times10^{-6}$	$6.291\,17\times10^{-6}$	...	21	1.10	2.41
0.840 374	$8.194\,03\times10^{-6}$	$4.640\,96\times10^{-5}$	4.643×10^{-5}	21	1.11	2.20
0.902 195	$6.386\,63\times10^{-5}$	$3.138\,53\times10^{-4}$	3.142×10^{-4}	21	1.30	2.32
1.000 02	$5.123\,40\times10^{-4}$	$2.049\,28\times10^{-3}$	2.049×10^{-3}	21	1.22	1.87
1.188 00	$5.000\,00\times10^{-3}$	1.41709×10^{-2}	1.419×10^{-2}	15	1.35	1.52
1.647 57	$6.400\,00\times10^{-2}$	$9.430\,88\times10^{-2}$	9.431×10^{-2}	15	1.70	1.50

[a] Obtained by linear or quadratic interpolation from Table I of Wallis *et al.* (Ref. 14).

[b] With factored determinant (see Ref. 20). (The last two digits found for $D_{\min}$ in Ref. 20 are not correct.)

TABLE II. Energy eigenvalues λ and optimized variational parameter α obtained with high-D expansion (3) and dipole charge $q=e$.

D (ea_0)	$-\mu$	$-\lambda$ (Ry) This calculation	$-\lambda$ (Ry) Wallis *et al.*[14]	Rank	α (For rank shown)
2	0.176 264	0.176 264	0.176 266	21	1.616
3	0.855 681	0.380 303	0.380 302	21	2.981
4	2.066 35	0.516 588	0.516 587	15	4.03
5	3.794 35	0.607 096	0.607 097	10	4.99
6	6.031 35	0.670 150	0.670 150	10	6.12
7	8.773 19	0.716 179	0.716 179	10	7.12
8	12.017 8	0.751 113	0.751 112	6	7.809
9	15.764 1	0.778 474	0.778 472	6	8.799
10	20.011 4	0.800 456	0.800 455	6	9.800
15	48.755 0	0.866 756	0.866 756	6	14.872
20	90.002 8	0.900 028	0.900 028	3	19.90
25	143.752	0.920 013	0.920 011	3	24.58
30	210.001	0.933 338	0.933 339	3	29.60
40	380.001	0.950 003	...	3	39.71
50	600.000	0.960 000	...	1	50.00
100	2450.00	0.980 000	...	1	100.0
250	1.55×10^{4}	0.992	...	1	250.0
400	3.98×10^{4}	0.995	...	1	400.0

gence with increasing rank in the region $D\sim 1.65$ to $D\sim 2$. At $D=2$, a 21-term high-D function gives the energy eigenvalue slightly better – six parts in the sixth digit – than the low-D function of the same rank. At $D=1$, on the other hand, the convergence of the high-D expansion is very poor. As seen below in Fig. 6, the electronic charge density in this region of D loses its hydrogenic character of rapid decrease away from the positive charge and assumes a much flatter distribution, characteristic of the dipole with its critical value, $D_{\mathrm{min}}=0.6393$.

The electronic probability density, $|\psi(\xi,\eta)|^2$, was calculated with the coefficients in Tables III and IV. Figure 2 is a contour map, showing the positions at which $\psi^2(=|\psi|^2)$ is equal to inverse powers of 10 when $D=10$. The vertical z axis shows the distance along the axis of the dipole, having charges located at $z=\pm 5$, and the horizontal ρ axis gives the perpen-

TABLE III. Coefficients in low-D expansion (2) of trial functions. The column headings give the dipole moment D. (Dipole charge: $q=e$).

C_{pq}	0.6670	0.674 65	0.602 72	0.732 65	0.740 99	0.764 49
C_{00}	1.02319×10^{-9}	8.41227×10^{-8}	6.80160×10^{-6}	1.87080×10^{-4}	5.53976×10^{-4}	1.60324×10^{-3}
C_{01}	-6.41480×10^{-10}	-5.32521×10^{-8}	-4.40743×10^{-6}	-1.26000×10^{-4}	-3.80941×10^{-4}	-1.13295×10^{-3}
C_{10}	6.41043×10^{-15}	5.14399×10^{-12}	3.96626×10^{-9}	5.83018×10^{-7}	2.97015×10^{-6}	1.42153×10^{-5}
C_{02}	1.39202×10^{-10}	1.17108×10^{-8}	9.84756×10^{-7}	2.93584×10^{-5}	9.07882×10^{-5}	2.78143×10^{-4}
C_{11}	-4.03870×10^{-15}	-3.27440×10^{-12}	-2.57437×10^{-9}	-3.93224×10^{-7}	-2.04538×10^{-6}	-1.00605×10^{-5}
C_{20}	2.86450×10^{-22}	4.58585×10^{-18}	6.90473×10^{-14}	9.90231×10^{-11}	1.09576×10^{-9}	1.13143×10^{-8}
C_{03}	-1.49140×10^{-11}	-1.25652×10^{-9}	-1.12939×10^{-7}	-3.51370×10^{-6}	-1.11084×10^{-5}	-3.50045×10^{-5}
C_{12}	8.21247×10^{-16}	6.59525×10^{-13}	5.79354×10^{-10}	9.15606×10^{-8}	4.85404×10^{-7}	2.44842×10^{-6}
C_{21}	-1.72150×10^{-22}	-2.75100×10^{-18}	-4.42750×10^{-14}	-6.61370×10^{-11}	-7.47100×10^{-10}	-7.92336×10^{-9}
C_{30}	1.23826×10^{-30}	8.66862×10^{-25}	4.98105×10^{-19}	1.09141×10^{-14}	2.78298×10^{-13}	6.00560×10^{-12}
C_{04}	1.10432×10^{-12}	9.75388×10^{-11}	7.40330×10^{-9}	2.38389×10^{-7}	7.69712×10^{-7}	2.50054×10^{-6}
C_{13}	-1.15140×10^{-16}	-9.62860×10^{-14}	-5.89540×10^{-11}	-9.69137×10^{-9}	-5.28339×10^{-8}	-2.78403×10^{-7}
C_{22}	5.46145×10^{-23}	9.85215×10^{-19}	9.24623×10^{-15}	1.52683×10^{-11}	1.81113×10^{-10}	2.04172×10^{-9}
C_{31}	-9.72350×10^{-31}	-6.81640×10^{-25}	-3.27080×10^{-19}	-7.38740×10^{-15}	-1.92540×10^{-13}	-4.28990×10^{-12}
C_{40}	5.97061×10^{-40}	1.79861×10^{-32}	2.49654×10^{-25}	2.24859×10^{-20}	-9.00470×10^{-20}	-1.08600×10^{-16}
C_{05}	...	...	-4.11990×10^{-10}	-1.43203×10^{-8}	-4.78159×10^{-8}	-1.61214×10^{-7}
C_{14}	...	...	5.57057×10^{-12}	9.85113×10^{-10}	5.53695×10^{-9}	3.00710×10^{-8}
C_{23}	...	...	-1.93960×10^{-15}	-3.28930×10^{-12}	-3.83480×10^{-11}	-4.11860×10^{-10}
C_{32}	...	...	8.69300×10^{-20}	1.81651×10^{-15}	4.58870×10^{-14}	9.79650×10^{-13}
C_{41}	...	...	-1.72230×10^{-25}	-2.19280×10^{-20}	-3.13400×10^{-19}	6.79650×10^{-17}
C_{50}	...	...	2.20323×10^{-32}	1.72919×10^{-25}	2.24373×10^{-23}	7.79253×10^{-22}

C_{pq}	0.797 368	0.840 374	0.902 195	1.000 02	1.188 00	1.647 57
C_{00}	4.50037×10^{-3}	1.13354×10^{-2}	2.96957×10^{-2}	6.16712×10^{-2}	1.30733×10^{-1}	2.82724×10^{-1}
C_{01}	-3.29818×10^{-3}	-8.69168×10^{-3}	-2.41770×10^{-2}	-5.46855×10^{-2}	-1.33410×10^{-1}	-3.71080×10^{-1}
C_{10}	6.51627×10^{-5}	2.40318×10^{-4}	3.88507×10^{-4}	1.69273×10^{-3}	7.91603×10^{-3}	-1.69758×10^{-2}
C_{02}	8.42223×10^{-4}	2.33100×10^{-3}	6.91062×10^{-3}	1.71522×10^{-2}	4.86076×10^{-2}	1.83918×10^{-1}
C_{11}	-4.78899×10^{-5}	-1.84657×10^{-4}	-3.18681×10^{-4}	-1.52001×10^{-3}	-8.02142×10^{-3}	2.23072×10^{-2}
C_{20}	1.20984×10^{-7}	8.68274×10^{-7}	-7.12493×10^{-7}	1.47508×10^{-5}	3.19286×10^{-4}	4.09622×10^{-4}
C_{03}	-1.10173×10^{-4}	-3.19239×10^{-4}	-1.00952×10^{-3}	-2.74734×10^{-3}	-8.97716×10^{-3}	-4.89149×10^{-2}
C_{12}	1.21063×10^{-5}	4.88468×10^{-5}	9.15759×10^{-5}	4.89058×10^{-4}	$3.13595\ 10^{-3}$	-1.09963×10^{-2}
C_{21}	-8.70254×10^{-8}	-6.56091×10^{-7}	6.39748×10^{-7}	-1.14812×10^{-5}	-3.23453×10^{-4}	-5.02101×10^{-4}
C_{30}	1.18700×10^{-10}	1.15210×10^{-9}	-2.23480×10^{-10}	-1.70236×10^{-7}	-1.60954×10^{-6}	-6.33671×10^{-6}
C_{04}	8.19184×10^{-6}	2.51633×10^{-5}	9.07401×10^{-5}	2.68923×10^{-4}	1.30488×10^{-3}	7.21738×10^{-3}
C_{13}	-1.45082×10^{-6}	-6.39060×10^{-6}	-1.32096×10^{-5}	-8.40555×10^{-5}	-8.19085×10^{-4}	2.38293×10^{-3}
C_{22}	2.34181×10^{-8}	1.89499×10^{-7}	-1.91982×10^{-7}	2.74214×10^{-6}	1.05307×10^{-4}	1.88808×10^{-4}
C_{31}	-9.16330×10^{-11}	-9.46840×10^{-10}	-1.74840×10^{-10}	1.09760×10^{-7}	8.99382×10^{-7}	4.05598×10^{-6}
C_{40}	-2.57810×10^{-15}	-2.52800×10^{-13}	8.96648×10^{-13}	6.38234×10^{-10}	1.02979×10^{-11}	5.70809×10^{-8}
C_{05}	-5.54058×10^{-7}	-1.77963×10^{-6}	-5.90211×10^{-6}	-2.04145×10^{-5}	...	...
C_{14}	1.64649×10^{-7}	7.37649×10^{-7}	9.98298×10^{-7}	8.66910×10^{-6}	...	...
C_{23}	-4.55460×10^{-9}	-3.28563×10^{-8}	2.36285×10^{-8}	-1.69905×10^{-7}	...	...
C_{32}	2.08919×10^{-11}	1.86825×10^{-10}	8.47278×10^{-11}	-1.82549×10^{-8}	...	...
C_{41}	5.33322×10^{-15}	3.19703×10^{-13}	-1.21380×10^{-13}	-2.27320×10^{-10}	...	...
C_{50}	-1.39570×10^{-18}	-1.15680×10^{-16}	-3.36920×10^{-16}	-8.43580×10^{-13}	...	...

dicular distance from the dipole axis. Distances are in atomic units. The maximum value, $\psi^2 = 0.3178$, of the probability density occurs at the position of the positive charge. The contours are approximately circular about this point, the system being equivalent to a hydrogen atom perturbed by a stationary electron at a distance $10a_0$ from the proton. The contours show some distortion in the positive z direction, toward the upper region of space. Figures 3, 4, and 5 show additional contours.

As the critical moment $D_{\text{min}} = 0.6393$ is approached, the probability density shifts into the upper region of space ($\eta < 0$), extending out to great distances there.

In Fig. 6 we have plotted on a log-log scale profiles of ψ^2 along the z axis for a number of values of dipole moment. The hydrogenic character of the probability density when D is large is demonstrated by the sharpness of the peaks at the locations of the positive dipole charges. The transition to the flat, dipole distribution occurs in the region from about $D = 3$ to $D = 1$.[32] A striking feature of Fig. 6 is the precipitous drop in the magnitude of ψ^2 in the vicinity of the dipole as the critical value $D_{\text{min}} = 0.6393$ is approached. The peak value of ψ^2 decreases by eight orders of magnitude in going from $D = 0.69272$ to $D = 0.6670$, as does the binding energy; the change in dipole moment is ~4%.

A number of mean values calculated with the wave functions from Tables III and IV are given in Table V. These values approach the correct hydrogenic

TABLE IV. Coefficients in high-D expansion (3) of trial functions. The column headings give the dipole moment D. (Dipole charge: $q = e$).

C_{pq}	2	3	4	5	6	7	8	9
C_{00}	$2.758\,03\times10^{-1}$	$3.641\,33\times10^{-1}$	$4.074\,46\times10^{-1}$	$4.182\,86\times10^{-1}$	$4.388\,20\times10^{-1}$	$4.237\,33\times10^{-1}$	$4.576\,51\times10^{-1}$	$4.660\,84\times10^{-1}$
C_{01}	$-1.959\,84\times10^{-1}$	$-2.201\,64\times10^{-1}$	$-2.181\,03\times10^{-1}$	$-2.171\,31\times10^{-1}$	$-1.947\,33\times10^{-1}$	$-1.992\,24\times10^{-1}$	$-2.464\,09\times10^{-1}$	$-2.464\,07\times10^{-1}$
C_{10}	$-3.672\,27\times10^{-2}$	$-4.451\,65\times10^{-2}$	$-5.456\,77\times10^{-2}$	$-4.299\,11\times10^{-2}$	$-3.582\,01\times10^{-2}$	$1.422\,39\times10^{-2}$	$-1.070\,58\times10^{-1}$	$-1.153\,55\times10^{-1}$
C_{02}	$-3.251\,99\times10^{-4}$	$-5.122\,95\times10^{-2}$	$-9.093\,31\times10^{-2}$	$-8.715\,02\times10^{-2}$	$-1.163\,43\times10^{-1}$	$-1.281\,82\times10^{-1}$	$-8.154\,08\times10^{-2}$	$-8.069\,37\times10^{-2}$
C_{11}	$2.637\,90\times10^{-2}$	$2.123\,06\times10^{-2}$	$9.020\,18\times10^{-3}$	$-7.962\,81\times10^{-3}$	$-2.550\,58\times10^{-2}$	$-2.481\,58\times10^{-2}$	$-2.083\,12\times10^{-3}$	$-1.456\,94\times10^{-5}$
C_{20}	$2.237\,22\times10^{-2}$	$4.775\,03\times10^{-2}$	$6.841\,38\times10^{-2}$	$4.004\,56\times10^{-2}$	$4.641\,99\times10^{-2}$	$7.122\,10\times10^{-3}$	$4.525\,86\times10^{-2}$	$4.682\,10\times10^{-2}$
C_{03}	$6.493\,04\times10^{-3}$	$6.311\,49\times10^{-3}$	$2.596\,19\times10^{-3}$	$-8.345\,90\times10^{-3}$	$-2.086\,26\times10^{-2}$	$-2.443\,05\times10^{-2}$	...	...
C_{12}	$-2.310\,00\times10^{-4}$	$-1.452\,75\times10^{-4}$	$5.598\,63\times10^{-3}$	$-1.578\,26\times10^{-2}$	$-2.284\,51\times10^{-2}$	$-2.040\,70\times10^{-2}$	...	...
C_{21}	$-1.610\,94\times10^{-2}$	$-2.478\,53\times10^{-2}$	$-1.844\,21\times10^{-2}$	$-1.144\,84\times10^{-2}$	$-7.824\,97\times10^{-3}$	$-6.081\,57\times10^{-3}$	...	...
C_{30}	$-2.391\,27\times10^{-3}$	$-6.883\,39\times10^{-3}$	$-1.164\,94\times10^{-2}$	$2.175\,70\times10^{-4}$	$1.708\,85\times10^{-3}$	$1.111\,06\times10^{-2}$	...	...
C_{04}	$5.914\,82\times10^{-4}$	$3.687\,39\times10^{-3}$	$5.520\,78\times10^{-3}$	...	...	...	...	...
C_{13}	$-5.435\,99\times10^{-4}$	$2.542\,21\times10^{-4}$	$-1.092\,04\times10^{-3}$	...	...	...	...	...
C_{22}	$6.166\,87\times10^{-5}$	$-2.383\,98\times10^{-3}$	$-9.168\,26\times10^{-3}$	...	...	...	...	...
C_{31}	$1.774\,18\times10^{-3}$	$2.785\,80\times10^{-3}$	$-9.629\,71\times10^{-4}$	...	...	...	...	...
C_{40}	$2.098\,37\times10^{-4}$	$1.010\,06\times10^{-3}$	$1.820\,68\times10^{-3}$	...	...	...	...	...
C_{05}	$2.976\,10\times10^{-6}$	$8.526\,82\times10^{-4}$	...	...	...	...	...	...
C_{14}	$1.019\,14\times10^{-4}$	$8.415\,17\times10^{-4}$	...	...	...	...	...	...
C_{23}	$3.203\,08\times10^{-4}$	$4.134\,30\times10^{-4}$	...	...	...	...	...	...
C_{32}	$-7.015\,76\times10^{-6}$	$-3.561\,66\times10^{-4}$	...	...	...	...	...	...
C_{41}	$-1.613\,50\times10^{-4}$	$-4.346\,66\times10^{-4}$	...	...	...	...	...	...
C_{50}	$1.097\,76\times10^{-6}$	$-8.437\,94\times10^{-6}$	...	...	...	...	...	...

C_{pq}	10	15	20	25	30	40	50	100
C_{00}	$4.734\,92\times10^{-1}$	$4.990\,24\times10^{-1}$	$5.134\,74\times10^{-1}$	$5.199\,87\times10^{-1}$	$5.271\,98\times10^{-1}$	$5.362\,45\times10^{-1}$	$5.461\,73\times10^{-1}$	$5.641\,90\times10^{-1}$
C_{01}	$-2.440\,44\times10^{-1}$	$-2.177\,34\times10^{-1}$	$-2.026\,97\times10^{-1}$	$-1.383\,50\times10^{-1}$	$-1.296\,15\times10^{-1}$	$-9.521\,41\times10^{-2}$	...	...
C_{10}	$-1.209\,51\times10^{-1}$	$-1.253\,76\times10^{-1}$	$-1.296\,01\times10^{-1}$	$-9.424\,62\times10^{-2}$	$-9.268\,59\times10^{-2}$	$-6.728\,52\times10^{-2}$	...	...
C_{02}	$-8.048\,21\times10^{-2}$	$-8.208\,11\times10^{-2}$	$-8.056\,41\times10^{-2}$	...	...	...	...	...
C_{11}	$9.853\,11\times10^{-4}$	$1.095\,05\times10^{-4}$	$1.366\,28\times10^{-4}$	...	...	...	...	...
C_{20}	$4.844\,51\times10^{-2}$	$5.484\,67\times10^{-2}$	$5.826\,48\times10^{-2}$	...	...	...	...	...
C_{03}	...	...	...	...	...	...	...	...
C_{12}	...	...	...	...	...	...	...	...
C_{21}	...	...	...	...	...	...	...	...
C_{30}	...	...	...	...	...	...	...	...
C_{04}	...	...	...	...	...	...	...	...
C_{13}	...	...	...	...	...	...	...	...
C_{22}	...	...	...	...	...	...	...	...
C_{31}	...	...	...	...	...	...	...	...
C_{40}	...	...	...	...	...	...	...	...
C_{05}	...	...	...	...	...	...	...	...
C_{14}	...	...	...	...	...	...	...	...
C_{23}	...	...	...	...	...	...	...	...
C_{32}	...	...	...	...	...	...	...	...
C_{41}	...	...	...	...	...	...	...	...
C_{50}	...	...	...	...	...	...	...	...

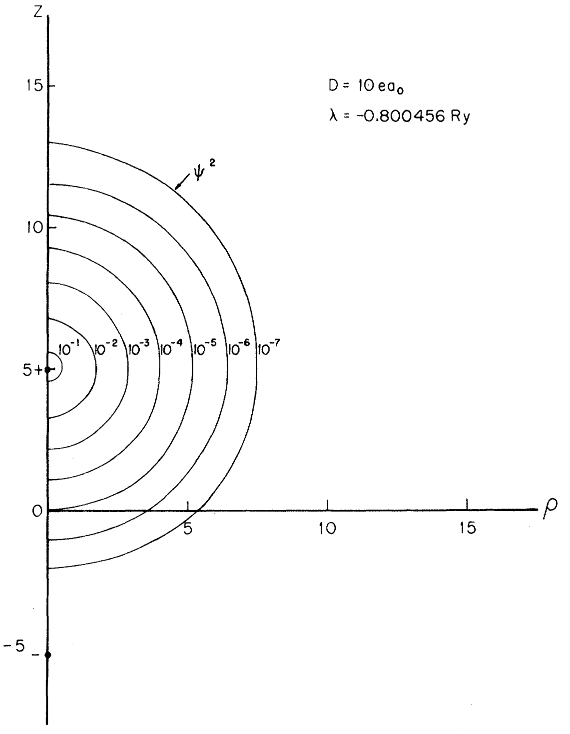

FIG. 2. Probability-density contours for $D = 10\ ea_0$. The dipole has charges ± e. Distances are in units of a_0.

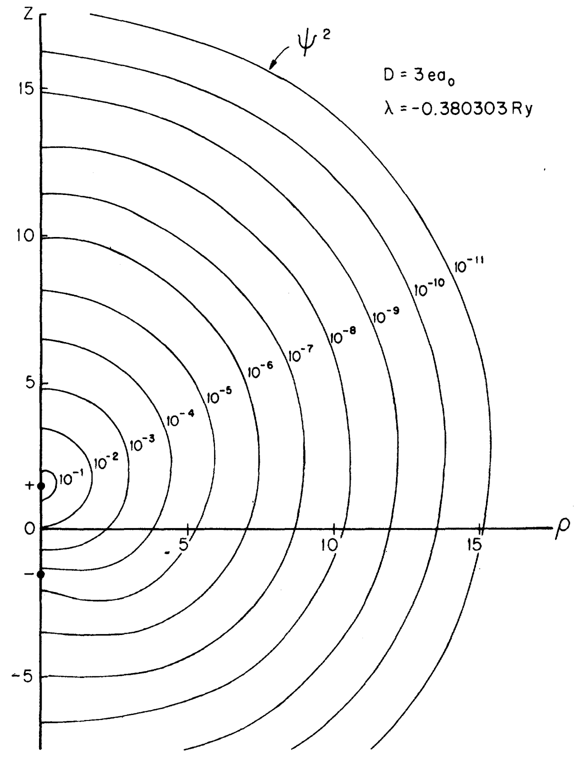

FIG. 3. Probability-density contours for $D = 3\ ea_0$. The dipole has charges ± e. Distances are in units of a_0.

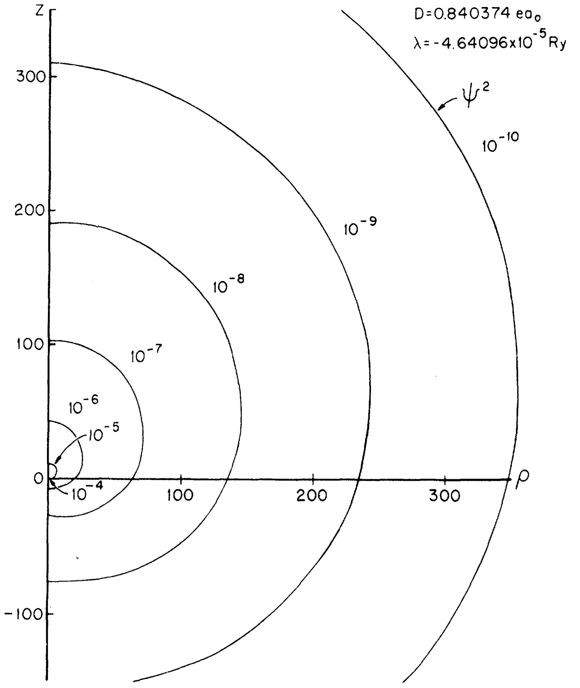

FIG. 4. Probability-density contours for $D = 0.840374\ ea_0$. The dipole has charges ± e. Distances are in units of a_0.

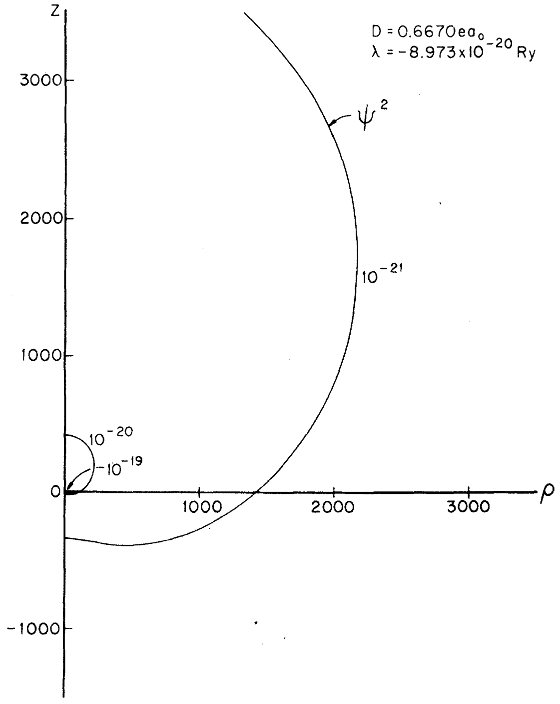

FIG. 5. Probability-density contours for $D = 0.6670\ ea_0$. The dipole has charges ± e. Distances are in units of a_0.

limits[33] as D becomes large. Figure 7 shows how the mean distance of the electron from the positive dipole charge ($q = e$) varies with dipole moment. When $D \sim 2$, the quantity $\langle r_1 \rangle$ is within a factor of 2 of its value $\frac{3}{2}$ for the isolated hydrogen atom. As we have already seen, between $D = 2$ and $D = 1$ the charge distribution changes dramatically and becomes extremely strongly dependent on D, as evidenced by the steep slope of the curve in Fig. 7.

ACKNOWLEDGMENT

The authors wish to thank Dr. W. R. Garrett for a number of helpful discussions.

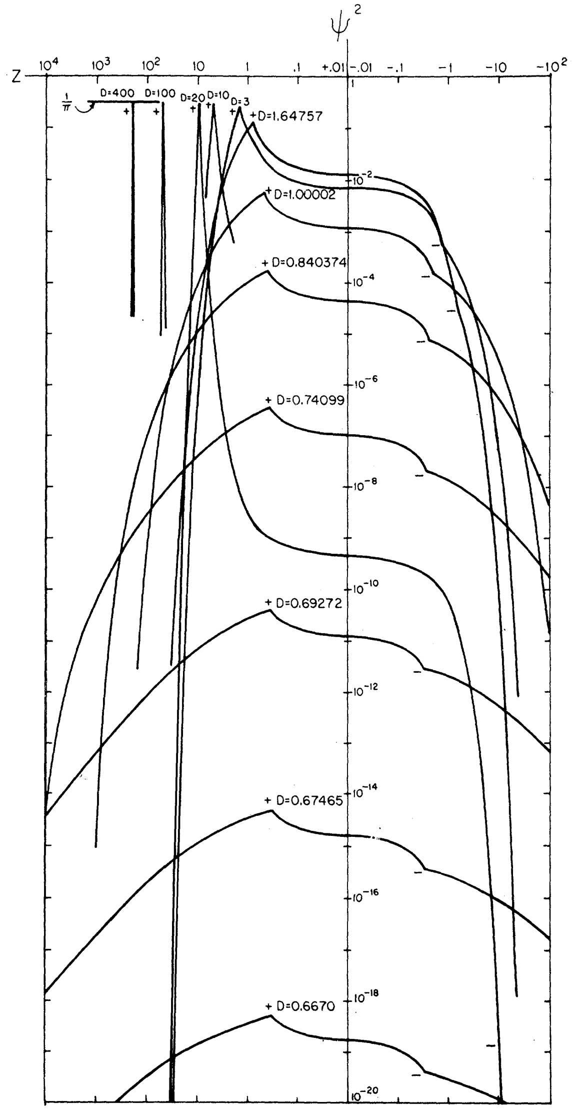

FIG. 6. Profiles of probability density along the dipole axis for a number of values of dipole moment.

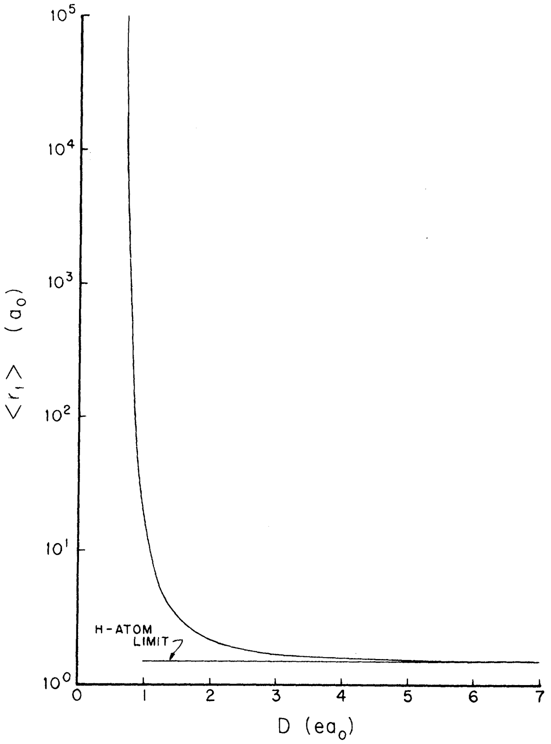

FIG. 7. Mean distance $\langle r_1 \rangle$ of the electron from the positive dipole charge ($q = e$) as a function of dipole moment D. (Atomic units).

TABLE V. Mean values of powers of r_1 and r_2 (see Fig. 1) in atomic units.

D (ea_0)	$\langle 1/r_1 \rangle$	$\langle 1/r_2 \rangle$	$\langle r_1 \rangle$	$\langle r_2 \rangle$	$\langle r_1^2 \rangle$	$\langle r_2^2 \rangle$
0.667 0	$1.988\,44 \times 10^{-9}$	$1.988\,44 \times 10^{-9}$	$1.680\,90 \times 10^{9}$	$1.680\,90 \times 10^{9}$	$6.025\,33 \times 10^{18}$	$6.025\,33 \times 10^{18}$
0.675 65	$1.631\,75 \times 10^{-7}$	$1.631\,75 \times 10^{-7}$	$1.854\,35 \times 10^{7}$	$1.854\,35 \times 10^{7}$	$6.841\,69 \times 10^{14}$	$6.841\,69 \times 10^{14}$
0.692 72	$1.276\,93 \times 10^{-5}$	$1.276\,84 \times 10^{-5}$	$2.231\,86 \times 10^{5}$	$2.231\,86 \times 10^{5}$	$9.420\,90 \times 10^{10}$	$9.420\,91 \times 10^{10}$
0.723 65	$3.601\,40 \times 10^{-4}$	$3.597\,19 \times 10^{-4}$	$7.367\,61 \times 10^{3}$	$7.367\,89 \times 10^{3}$	$9.540\,85 \times 10^{7}$	$9.541\,27 \times 10^{7}$
0.740 99	$1.074\,28 \times 10^{-3}$	$1.071\,19 \times 10^{-3}$	$2.405\,22 \times 10^{3}$	$2.405\,52 \times 10^{3}$	$9.963\,40 \times 10^{6}$	$9.964\,83 \times 10^{6}$
0.764 49	$3.153\,58 \times 10^{-3}$	$3.131\,70 \times 10^{-3}$	$7.947\,04 \times 10^{2}$	$7.950\,17 \times 10^{2}$	$1.069\,92 \times 10^{6}$	$1.070\,41 \times 10^{6}$
0.797 368	$9.056\,08 \times 10^{-3}$	$8.908\,68 \times 10^{-3}$	$2.668\,08 \times 10^{2}$	$2.671\,43 \times 10^{2}$	$1.191\,61 \times 10^{5}$	$1.193\,40 \times 10^{5}$
0.840 374	$2.310\,83 \times 10^{-2}$	$2.231\,24 \times 10^{-2}$	$1.003\,55 \times 10^{2}$	$1.007\,20 \times 10^{2}$	$1.665\,92 \times 10^{4}$	$1.673\,27 \times 10^{4}$
0.902 195	$5.568\,99 \times 10^{-2}$	$5.184\,51 \times 10^{-2}$	$3.978\,01 \times 10^{1}$	$4.018\,95 \times 10^{1}$	$2.602\,99 \times 10^{3}$	$2.635\,73 \times 10^{3}$
1.000 02	$1.292\,28 \times 10^{-1}$	$1.120\,49 \times 10^{-1}$	$1.617\,23 \times 10^{1}$	$1.665\,27 \times 10^{1}$	$4.177\,62 \times 10^{2}$	$4.335\,51 \times 10^{2}$

TABLE V (*continued*)

D (ea_0)	$\langle 1/r_1\rangle$	$\langle 1/r_2\rangle$	$\langle r_1\rangle$	$\langle r_2\rangle$	$\langle r_1^2\rangle$	$\langle r_2^2\rangle$
1.188 00	$2.965\,08\times 10^{-1}$	$2.219\,46\times10^{-1}$	6.546 33	7.165 79	$6.657\,05\times10^{1}$	$7.510\,94\times10^{1}$
1.647 57	$6.184\,81\times10^{-1}$	$3.405\,37\times10^{-1}$	2.821 10	3.786 65	$1.183\,49\times10^{1}$	$1.830\,59\times10^{1}$
2	$7.591\,62\times10^{-1}$	$3.485\,99\times10^{-1}$	2.191 31	3.428 82	6.963 32	$1.403\,46\times10^{1}$
3	$9.235\,67\times10^{-1}$	$2.918\,30\times10^{-1}$	1.689 37	3.740 03	3.960 64	$1.525\,78\times10^{1}$
4	$9.703\,78\times10^{-1}$	$2.347\,66\times10^{-1}$	1.572 29	4.492 26	3.360 59	$2.125\,98\times10^{1}$
5	$9.866\,74\times10^{-1}$	$1.932\,94\times10^{-1}$	1.532 66	5.362 38	3.162 92	$2.977\,72\times10^{1}$
6	$9.932\,76\times10^{-1}$	$1.633\,13\times10^{-1}$	1.516 58	6.283 01	3.083 02	$4.047\,87\times10^{1}$
7	$9.962\,85\times10^{-1}$	$1.410\,12\times10^{-1}$	1.509 22	7.230 14	3.046 53	$5.327\,06\times10^{1}$
8	$9.978\,00\times10^{-1}$	$1.239\,07\times10^{-1}$	1.505 44	8.192 78	3.028 17	$6.811\,53\times10^{1}$
9	$9.986\,19\times10^{-1}$	$1.104\,25\times10^{-1}$	1.503 42	9.165 15	3.017 82	$8.499\,32\times10^{1}$
10	$9.990\,92\times10^{-1}$	$9.954\,88\times10^{-2}$	1.502 25	$1.014\,41\times10^{1}$	3.011 80	$1.038\,95\times10^{2}$
15	$9.998\,21\times10^{-1}$	$6.657\,73\times10^{-2}$	1.500 44	$1.508\,65\times10^{1}$	3.002 40	$2.285\,99\times10^{2}$
20	$9.999\,43\times10^{-1}$	$4.997\,18\times10^{-2}$	1.500 14	$2.006\,12\times10^{1}$	3.000 78	$4.034\,50\times10^{2}$
25	$9.999\,79\times10^{-1}$	$3.998\,96\times10^{-2}$	1.499 89	$2.504\,65\times10^{1}$	2.999 25	$6.283\,25\times10^{2}$
30	$9.999\,90\times10^{-1}$	$3.332\,83\times10^{-2}$	1.499 92	$3.003\,78\times10^{1}$	2.999 49	$9.032\,70\times10^{2}$
40	$9.999\,97\times10^{-1}$	$2.499\,84\times10^{-2}$	1.499 98	$4.002\,75\times10^{1}$	2.999 88	$1.603\,20\times10^{3}$
50	1.000 00	$2.000\,00\times10^{-2}$	1.500 00	$5.002\,00\times10^{1}$	3.000 00	$2.503\,00\times10^{3}$
100	1.000 00	$1.000\,00\times10^{-2}$	1.500 00	$1.000\,10\times10^{2}$	3.000 00	$1.000\,30\times10^{4}$

---

*Research sponsored in part by the U. S. Atomic Energy Commission under contract with Union Carbide Corporation.

†Central Data Processing Center, Oak Ridge Gaseous Diffusion Plant.

‡U. S. National Research Council Senior Postdoctoral Resident Research Associate, supported by the National Aeronautics and Space Administration; on leave from The University of Tennessee.

[1] S. Altshuler, Phys. Rev. 107, 114 (1957).

[2] M. Shimizu, J. Phys. Soc. Japan 18, 811 (1963).

[3] M. H. Mittleman and R. E. von Holdt, Phys. Rev. 140, A726 (1965).

[4] J. E. Turner and K. Fox, Oak Ridge National Laboratory Report No. ORNL-3895, 1965 (unpublished).

[5] J. E. Turner, Phys. Rev. 141, 21 (1966).

[6] Y. Itikawa, Phys. Letters 24A, 495 (1967).

[7] J. M. Lévy-Leblond, Phys. Rev. 153, 1 (1967).

[8] O. H. Crawford, J. Chem. Phys. 47, 1100 (1967).

[9] O. H. Crawford, A. Dalgarno, and P. B. Hays, Mol. Phys. 13, 181 (1967).

[10] K. Takayanagi and Y. Itikawa, J. Phys. Soc. Japan 24, 160 (1968).

[11] J. M. Lévy-Leblond and J. P. Provost, Phys. Letters 26B, 104 (1968).

[12] R. Stratton, J. Phys. Chem. Solids 23, 1011 (1962).

[13] L. Pincherle, Proc. Phys. Soc. (London) A64, 648 (1951).

[14] R. F. Wallis, R. Herman, and H. W. Milnes, J. Mol. Spectry. 4, 51 (1960).

[15] G. S. Hurst, L. B. O'Kelly, and J. A. Stockdale, Nature 195, 66 (1962).

[16] G. S. Hurst, J. A. Stockdale, and L. B. O'Kelly, J. Chem. Phys. 38, 2572 (1963).

[17] K. Fox and J. E. Turner, Am. J. Phys. 34, 606 (1966).

[18] K. Fox and J. E. Turner, J. Chem. Phys. 45, 1142 (1966).

[19] M. H. Mittleman and V. P. Myerscough, Phys. Letters 23, 545 (1966).

[20] J. E. Turner and K. Fox, Phys. Letters 23, 547 (1966).

[21] W. B. Brown and R. E. Roberts, J. Chem. Phys. 46, 2006 (1967).

[22] Dr. H. B. Snodgrass, presently at the University of California, Berkeley, recently called our attention to the work of A. S. Wightman, Phys. Rev. 77, 521 (1949), in which the effect of the presence of a slow negative pion or muon on electronic binding in the hydrogen molecule and in the hydrogen atom is discussed. Wightman's calculations show that an electron cannot be bound when the π-H$^+$ or μ-H$^+$ separation is less than $0.639a_0$. Wightman references an earlier paper by E. Fermi and E. Teller, Phys. Rev. 72, 399 (1947) on negative π- and μ-capture in matter, in which the following statement is made with no further elucidation: "In the special case of mesotron capture by the hydrogen atom, it is found that when the mesotron approaches the nucleus to a distance of 0.639 Bohr radii, the binding energy of the electron becomes zero." This is, to our knowledge, the earliest reference to this particular constant, rediscovered recently in molecular physics as the minimum dipole moment needed to bind an electron (Refs. 7, 19, 20, 21).

[23] J. A. D. Stockdale, L. G. Christophorou, J. Turner, and V. E. Anderson, Phys. Letters 25A, 519 (1967).

[24] C. A. Coulson and M. Walmsley, Proc. Phys. Soc. (London) 91, 31 (1967).

[25] O. H. Crawford, Proc. Phys. Soc. (London) 91, 279 (1967).

[26] Hereafter we shall express dipole moments in units of ea_0 without showing these symbols.

[27] J. E. Turner and K. Fox, J. Phys. A: Proc. Phys. Soc. (London) 1, 118 (1968).

[28] K. Fox, J. Phys. A: Proc. Phys. Soc. (London) 1, 124 (1968).

[29] For convenience and simplicity of notation, we shall use the same symbols α, t, and C_{pq} in the different trial functions.

[30] J. E. Turner, V. E. Anderson, and K. Fox, Oak Ridge National Laboratory Report No. ORNL-4297 (unpublished).

[31] The angular momentum of the electron about the z axis being zero in the ground state, we have omitted this operator from Eq. (5).

[32] In plotting $\log z$ along the abscissa, the values $z = \pm 0.01$ were given the same position. The values of ψ^2 at these two points were very nearly equal.

[33] H. A. Bethe and E. E. Salpeter, *Quantum Mechanics of One- and Two-Electron Atoms* (Academic Press Inc., New York, 1957), p. 17.

PHYSICAL REVIEW VOLUME 174, NUMBER 1 5 OCTOBER 1968

Magnetic Parameters for the Configuration f^3 †

Hannah Crosswhite, H. M. Crosswhite, and B. R. Judd
The Johns Hopkins University, Baltimore, Maryland 21218

(Received 5 June 1968)

The energy-level schemes of several atomic configurations f^3 are analyzed in terms of effective operators. These include all possible Hermitian two-electron scalar operators and six three-body spin-independent scalar operators. This collection of operators allows for spin-spin and spin-other-orbit interactions as well as for the most important effects of configuration interaction. Several alterations and extensions are suggested for the terms of Pr III $4f^3$. The positions of the free-ion levels of Nd IV $4f^3$ and Er IV $4f^{11}$ are inferred from the crystal spectra of Nd^{3+} in $LaCl_3$, and analyses with restricted sets of operators are carried out.

I. INTRODUCTION

It is often useful to introduce effective operators in the analysis of the energy-level systems of electronic configurations for free atoms and ions. This method avoids the construction of accurate eigenfunctions. Instead, the eigenfunctions of a particular configuration under study are assumed pure, and the responsibility for getting a good fit with experiment rests with the choice of an effective Hamiltonian. It is convenient to express this as a sum of coupled tensors, for then a wide variety of effects can be taken into account by comparatively few operators. The coefficients of these operators can be treated as parameters, through which the experimental data can be represented in a more concise and significant form. This approach works best for configurations that are comparatively isolated from their neighbors.

Considerable work has been carried out by Shadmi[1] on the configurations $(d+s)^N$. Our own interest in the spectra of the doubly and triply ionized rare earths has led us to investigate the configurations f^N. These are more appealing from a theoretical standpoint, because there are many more levels to be fitted. The only difficulty is in finding experimental data that have been analyzed extensively enough. Preliminary analyses for several configurations of the type f^N have been reported recently.[2] Although only partial-term schemes are known in some cases, it was found to be highly desirable to introduce an operator that would represent magnetic interactions between the f electrons. The success of this approach has encouraged us to attempt an analysis of several $4f^3$ species in which the number of experimentally determined levels makes it feasible to go beyond the conventional analysis and include operators that represent not only the direct magnetic interactions but also certain kinds of configuration interaction. We shall pay particular attention to the Pr III free-ion levels of Sugar.[3]

II. EFFECTIVE OPERATORS

A straightforward first-order analysis of the levels of a configuration f^N involves the Slater parameters F^k (where $k = 0$, 2, 4, and 6) and the spin-orbit coupling constant ζ. To allow for two-electron excitations (as well as certain electrostatic shielding effects and the magnetic orbit-orbit interaction), the three parameters α, β, and γ are required. Rajnak and Wybourne[4,5] introduced certain scalar three-electron operators to take into account single-electron excitations; it was shown later[6] that a complete parametrization is possible with just six parameters T^k. The inclusion of magnetic spin-spin and spin-other-orbit interactions introduces three parameters M^k (where $k = 0$, 2, and 4). Rather than treat these interactions as they stand, it is highly advantageous to decompose them into parts that have irreducible representations of certain continuous Lie groups as their labels. Four operators z_i $(1 \leq i \leq 4)$ are required for the spin-spin interaction,[7] and ten $(5 \leq i \leq 14)$ for the spin-other-orbit interaction.[2] Of the latter, z_{13} has matrix elements proportional to the ordinary spin-orbit interaction, and a linear relationship exists that allows us to replace z_{12} and z_{14} by a combined operator z_c, where, for the states of f^2, the equivalence

$$z_c \equiv (13/3)z_{12} - 40z_{13} + (4/3)z_{14}$$

is valid. In addition to satisfying many selection rules, the operators z_i are effective operators